

INTERNAL MOTIONS IN H II REGIONS. XI. THE EMISSION NEBULA SHARPLESS 206

P. Pişmiş and I. Hasse

Instituto de Astronomía
Universidad Nacional Autónoma de México
Received 1981 December 15

RESUMEN

Se determinan velocidades radiales en 142 puntos de la región H II S206 con el método Fabry-Pérot fotográfico usando los reflectores con diámetro de 2.1 metros en San Pedro Mártir y de 1.0 metro en Tonantzintla. La velocidad del conjunto concuerda con determinaciones previas. Nuestras velocidades cubren las extensiones débiles al oeste de la nebulosa que no estaban determinadas a la fecha. El campo de velocidades es consistente con una expansión direccional de S206.

ABSTRACT

Radial velocities at 142 points are obtained on the H II region S206 by photographic Fabry-Pérot interferometry using the reflectors with apertures of 2.1 meters at San Pedro Mártir and 1-m at Tonantzintla. The overall velocity agrees with previous determinations. Our velocities cover the western faint extensions of the nebula not studied hitherto. The velocity field is consistent with a directional expansion of S206.

Key words: INTERFEROMETRY-FABRY PEROT – RADIAL VELOCITIES – H II REGIONS

I. INTRODUCTION

The galactic emission object Sharpless 206 (NGC 1491) has an extension of 50 arcmin on PSS red plates. It has been the subject of detailed studies; in the optical region and in the radio continuum by Deharveng *et al.* (1976), in radio recombination lines, and in H₂CO and HI absorption lines by Walmsley *et al.* (1975). Blair *et al.* (1975) have searched the region for CO with positive results while the search for H₂CO has given negative results (Lo and Burke 1973). A recent study of the electron temperature in S206 is made from radio recombination lines by Carral *et al.* (1980). A general conclusion drawn from these studies is that S206 is an evolved H II region.

In this paper we present the radial velocity field ob-

tained by photographic Fabry-Pérot interferometry. Our data span the western fainter extensions of S206 not studied previously.

II. THE OBSERVATIONS

We have used a focal reducer mounted at the Cassegrain focus of the 1-m reflector at the observatory in Tonantzintla and the 2.1 m at the observatory in San Pedro Mártir. The étalon employed has a free spectral range of 283 km s⁻¹ at H α . The interferograms are taken through a 10 Å halfwidth interference filter at H α and a one stage Varo image intensifier. Calibrations are made with interferograms of a hydrogen lamp. Table 1 lists the observational data. The content of the columns is self explanatory. The linear scale on the interferograms (or direct image) is 49 arcsec mm⁻¹ for the 2.1 meter mate-

TABLE 1
THE OBSERVATIONAL MATERIAL

Interferogram	Coordinates of Center (1980)		Average Radial Velocity (km s ⁻¹)	No. of measured points	V _{LSR} (km s ⁻¹)	Exposure time (min)	Date of Observation
	α	δ					
FI 530	4 ^h 01 ^m 46	+51°16'3	-27.15±5.67	19	-29.05	22	Oct. 20, 1978
FI 553	4 ^h 01 ^m 36	+51°16'2	-28.99±4.04	14	-30.89	30	Jan. 21, 1979
FI 558	4 ^h 01 ^m 39	+51°16'2	-21.69±5.82	29	-23.59	20	Jan. 23, 1979
FI 840	4 ^h 01 ^m 14	+51°16'1	-26.70±4.78	80	-28.60	30	Oct. 27, 1981

rial and $90 \text{ arcsec mm}^{-1}$ for the 1 meter material. A direct $\text{H}\alpha$ image of S206 is reproduced in Figure 1 (Plate); Figure 2 (Plate) is a direct image is $[\text{S II}]\lambda\lambda 6717\text{-}6730$ lines with a 15 Å width filter of the fainter western extension of S206 taken with the 2.1 m telescope. A sample interferogram in $\text{H}\alpha$ is given in Figure 3 (Plate).

The measurements of FI 530, 553 and 538 were performed on a Mann comparator at the Earth Observations Division of the NASA Johnson Space Center and FI 840 was measured on a positive enlargement. The accuracy of the latter measurement is satisfactory and may be considered comparable to those made with a comparator.

III. THE VELOCITY FIELD

Radial velocities were obtained at 142 points from the four interferograms listed in Table 1. In that table we also give the mean of all velocity points on each interferogram with their standard deviations. The general agreement between the different interferograms is quite satisfactory. (The smaller negative value of FI 558 is due

to the inclusion of the southern edge of S206 where the velocities are less negative (see Figure 4)). A combined discussion of the data can thus be safely made. Figure 4 is a display of the individual velocity points from the three interferograms taken with the 1 meter reflector. The velocity points on FI 840 from the 2.1 m reflector of the western fainter regions are closer together and therefore they have been displayed separately in Figure 5 at a larger scale.

A velocity field of S206 using also the Fabry-Pérot technique was obtained earlier by Deharveng *et al.* (1976). The general trend of our velocities agrees with their conclusion that there exists a gradient in the radial velocities from the southeast to the northwest in the sense that the velocities become larger in negative values towards the northwest. Deharveng *et al.* suggest further that there is no clear-cut correlation between velocity and optical features. We believe that a correlation does exist as will be shown below.

A confrontation of the velocity field with the morphology of S206 suggests a division of S206 into subregions as drawn in Figure 4. In that figure we have marked by a dashed line roughly the limit towards the west of the observations of Deharveng *et al.* To the east, however, their velocities extend farther than ours. The different subregions are marked by letters A to G, G being the background not included in the subregions. To bring out clearly the kinematics of the different parts of S206 we reproduce in Figure 6 the same scheme of the subregions as in Figure 4 inscribing in each area their

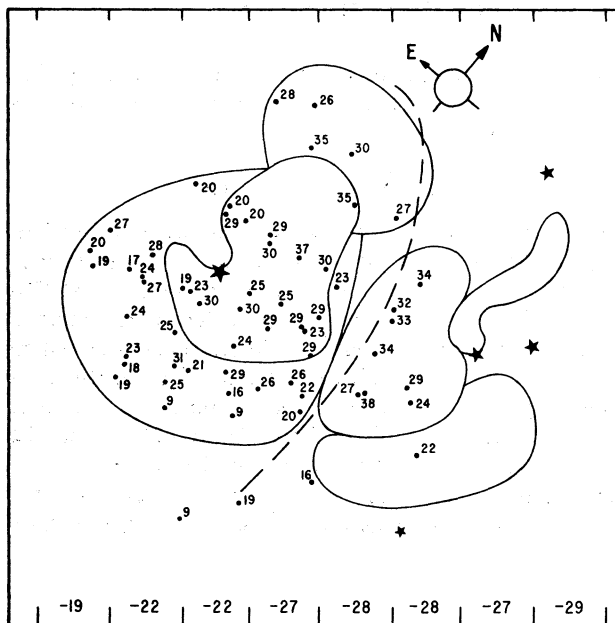


Fig. 4. A display of the velocity points with their velocities referred to the sun, obtained by the three interferograms taken with the 1.0 meter telescope at Tonantzintla observatory. The area is divided following the morphological details of the region of S206. These are marked by capital letters A to G. The dotted line is the western extent of the measurements by Deharveng *et al.* (1976). The parallel line segments at the bottom of the figure designate the columns within which the average velocities are given. This is intended to compare our gradient with that of Deharveng *et al.* (1976). The velocity points from the interferogram taken with the 2.1-m reflector are given separately in Figure 5. All velocities are referred to the sun and should be taken with a negative sign.

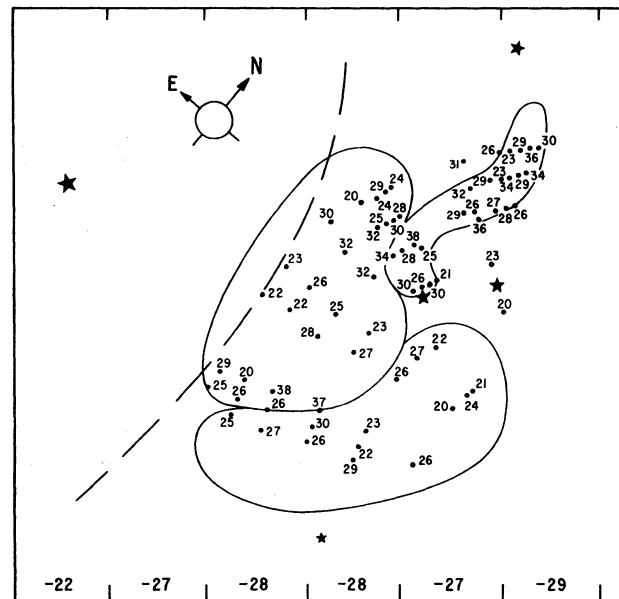


Fig. 5. A display of radial velocities obtained from interferogram FI 840 taken with the 2.1 meter telescope at San Pedro Mártir. Note the larger scale of the display. All velocities should be taken with a negative sign the sun. The LSR correction is -1.9 km s^{-1}

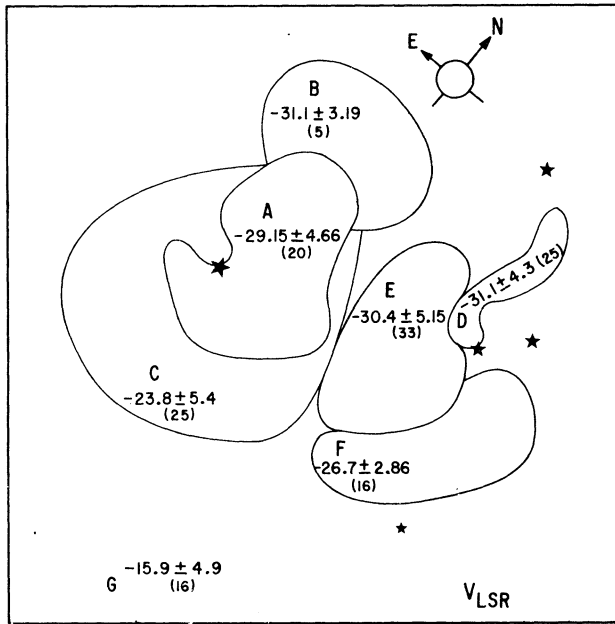


Fig. 6. The subdivisions of S206 are the same as in Figure 4. Here we have given for each subregion the mean LSR velocity and their standard deviations.

average velocities with standard deviations. There appears to exist a correlation between the location of the features and their mean radial velocities. The main body of S206 (which can be clearly seen on blue PSS plates) designated by A has a velocity larger than the southern fainter region enveloping it. To the west the faint regions show a slightly larger blue shift than region A and again the southern part shows lower negative velocity. The statement made by Deharveng *et al.* that the velocities become less negative towards the west in true up to the western limit of their observation but our data which as we have mentioned earlier extend farther westward than theirs show that the velocities definitely do not increase in negative values beyond the region covered by the dashed line; if at all, there is an increase. As regards the gradient of velocities, the averages in columns in direction as shown in Figure 4 run southeast to northwest as follows in km s^{-1} : $-19, -22, -22, -27, -28, -28, -27, -29$. This is to be compared with that of Deharveng *et al.* in km s^{-1} : $-22, -26, -27, -30, -32, -26, -28$.

No spurious effect is likely to cause the increase in negative velocities in the area at the extreme west; although it is true that the majority of the western velocity points are obtained from the 2.1 meter material (FI 840) while the eastern parts are from the three interferograms taken with the 1 m reflector, it can be easily seen from Table 1 that the mean radial velocity from FI 840 is comparable with the mean over the remaining three interferograms.

The average velocities of the different subregions in

Figure 6 suggests that the velocity field of S206 is consistent with an asymmetric expansion of the gas around the ionization source in the projected direction of roughly northwest-southeast with a line-of-sight component of the order of $6-7 \text{ km s}^{-1}$. The fainter regions are red shifted with respect to those of higher intensity. Deharveng *et al.* propose a more complicated model where the observed velocities are due to the streaming of ionized gas from the ionization front delineating the CO cloud to the northwest. Their model predicts a lower velocity of approach to the west of the main body of S206. However, our velocities as mentioned earlier do not show such a decrease; the slight decrease of the negative velocity past the main body of S206 is followed by an increase.

IV. THE SYSTEMIC VELOCITY OF S206

S206 is included in several lists of H II regions studied optically and by radio technique. The overall V_{LSR} of the earlier studies of radial velocities with their errors are given in Table 2. Column 1 refers to the technique and line used. Column 2 gives the V_{LSR} and the errors whenever available while column 3 lists the references. Our systemic LSR velocity, -27.9 km s^{-1} is contained in the range covered by those of Table 2. Due to the irregularities in the field and the circumstance that the different determinations may not cover the same areas of this rather extended nebula, a difference of about 10 km s^{-1} between the systemic velocities is not unexpected.

The distance obtained using $V_{\text{LSR}} = -27.9 \text{ km s}^{-1}$ and the Schmidt rotation curve is 2.5 kpc while the photometric distance of the main ionizing source of the nebula, the star BD + 50° 886 (O V), is estimated to be 3.6 kpc by Crampton and Georgelin (1975) and 3.0 by Moffet *et al.* (1979). The kinematic distance is thus smaller than the photometric one. Such a discrepancy is shown by almost all kinematic versus photometric distance of objects—H II regions or stars—in the Perseus arm (2nd galactic quadrant). The cause of this discrepancy lies most probably in the adoption of the Schmidt rotation curve which appears to deviate from the real rotation curve beyond the solar circle.

It is worth mentioning that the discrepancy changes its sign in the third galactic quadrant. This implies, as shown earlier by Pişmiş (1981), that the law of galactic rotation is not unique and that it is a function of direction. Thus the photometric distances seem to be the more reliable ones.

V. CONCLUSION

The radial velocities at 142 points on the H II region S206 (NGC 1491) have shown that the velocities are fairly well correlated with the structural details of the nebula. The radial velocity of the northwestern region (areas A, B and D) is blue shifted by 5 km s^{-1} with

TABLE 2
LIST OF LSR VELOCITIES OF S206 BY DIFFERENT AUTHORS

Observed line	V_{LSR} (km s^{-1})	Reference
H α	-33.3 \pm 3.9	Miller (1968)
H α	-29.1	Georgelin and Georgelin (1970)
H α	-24.0	Georgelin <i>et al.</i> (1973)
H α	-26.5	Deharveng <i>et al.</i> (1976)
H α	-27.9 \pm 5.6	this paper
H109 α	-26.3 \pm 0.8	Walmsley <i>et al.</i> (1975)
He109 α	-25.3 \pm 1.5	Walmsley <i>et al.</i> (1975)
H137 β	-26.1 \pm 1.2	Walmsley <i>et al.</i> (1975)
CO emission	-22.2, -22.9	Blair <i>et al.</i> (1975)
H137 β	-25.1 \pm 0.5	Churchwell <i>et al.</i> (1978)
H109 α	-26.5 \pm 0.1	Churchwell <i>et al.</i> (1978)
He109 α	-25.1 \pm 1.5	Churchwell <i>et al.</i> (1978)
H91 α	-25.7 \pm 0.2	Churchwell <i>et al.</i> (1978)
He91 α	-28.0 \pm 1.1	Churchwell <i>et al.</i> (1978)
H86 α	-26.6 \pm 0.2	Lichten <i>et al.</i> (1979)
He86 α	-29.6 \pm 0.5	Lichten <i>et al.</i> (1979)
H108 β	-29.7 \pm 0.8	Lichten <i>et al.</i> (1979)
BD+50° 886 (star)	-26.1 \pm 1.3	Crampton and Fisher (1974)

respect to the south and southeast (C and G). The radial velocity field appears to be consistent with the hypothesis that the nebula is expanding asymmetrically around the ionizing source BD + 50° 886.

We acknowledge the assistance of M. Moreno and A. Quintero in some stages of the observations. One of us (P.P.) is indebted to the NASA authorities for permission to use the Mann comparator at the Johnson Space Center. This is Contribution No. 62 of Instituto de Astronomía, UNAM.

REFERENCES

- Blair, G.N., Peters, W.L., and Van den Bout, P.A. 1975, *Ap. J. (Letters)*, 200, 161.
- Carral, P., Rodríguez, L.F., and Chaisson, E.J. 1981, *Astr. and Ap.*, 95, 388.
- Churchwell, E., Smith, L.F., Mathis, J., Mezger, P.G., and Huchtmeier, W. 1978, *Astr. and Ap.*, 70, 719.
- Crampton, D. and Fisher, W.A. 1974, *Pub. D.A.O.*, Vol. XIV, No. 2, p. 283.
- Crampton, D. and Georgelin, Y.M. 1975, *Astr. and Ap.*, 40, 317.
- Deharveng, L., Israel, F.P., and Maucherat, M. 1976, *Astr. and Ap.*, 48, 63.
- Georgelin, Y.P. and Georgelin, Y.M. 1970, *Astr. and Ap.*, 6, 349.
- Georgelin, Y.M., Georgelin, Y.P., and Roux, S. 1973, *Astr. and Ap.*, 25, 337.
- Lichten, S.M., Rodríguez, L.F., and Chaisson, E.J. 1979, *Ap. J.*, 229, 524.
- Lo, K.Y. and Burke, B.F. 1973, *Astr. and Ap.*, 26, 487.
- Moffat, A.F.J., FitzGerald, M.P., and Jackson, P.D. 1979, *Astr. and Ap. Suppl.*, 38, 197.
- Miller, J.S. 1968, *Ap. J.*, 151, 473.
- Pişmiş, P. 1981, *Rev. Mexicana Astron. Astrof.*, 6, 65.
- Walmsley, C.M. and Churchwell, E. 1975, *Astr. and Ap.*, 41, 121.

Ilse Hasse and Paris Pişmiş: Instituto de Astronomía, UNAM, Apartado Postal 70-264, 04510 México, D.F. México.

EMISSION NEBULA S206

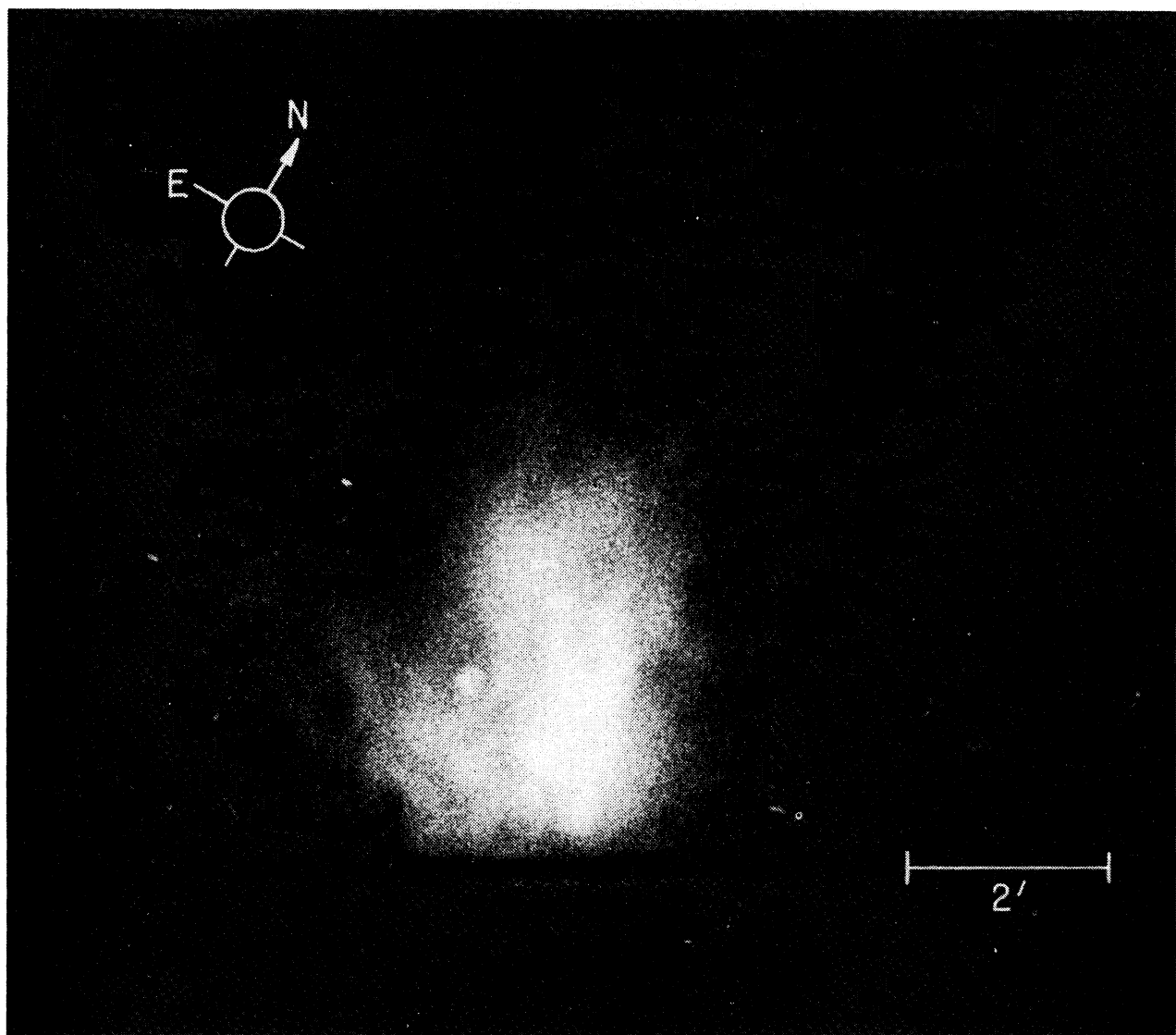


Fig. 1. An $H\alpha$ (10 Å halfwidth) photograph of S206 taken with a focal reducer attached to the 1-m reflector at Tonantzintla observatory. The nebula has fainter extensions towards the east not shown on the photograph. A one-stage Varo image intensifier is used in all the photographic material presented here.

P. PIŞMIŞ and I. HASSE (See page 209)

EMISSION NEBULA S206

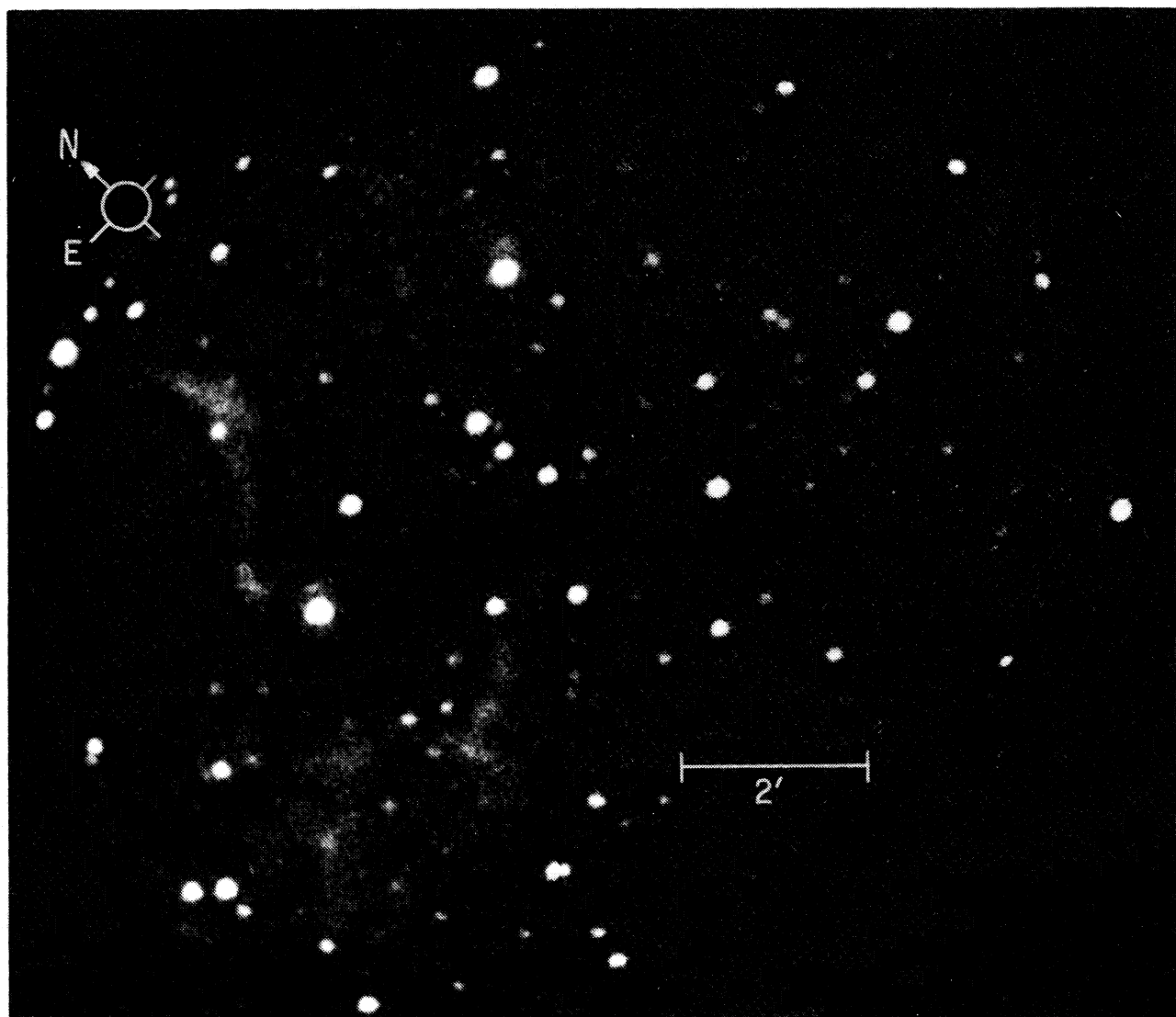


Fig. 2. An [S II] ($\lambda\lambda 6717-6730$) photograph of the faint features to the west of the main body of S206 taken with a focal reducer attached to the 2.1-m reflector at San Pedro Mártir.

P. PIŞMIŞ and I. HASSE (See page 209)